Chapter 4. Band Gap Narrowing in GaInN/GaAlN Surface Emission Diode

4.1 Introduction

In common with many areas of semiconductor physics, the study of heavily doped and highly excited semiconductor has benefited from the rapid progress in material science and the tools of physical investigation that has occurred in recent years. The highlight of this research period was the recognition that in many highly excited semiconductors a degenerate electron-hole liquid is formed at low temperatures, and electron-hole plasma at high temperatures. This guasimetallic state can only be described by including the effects of the screening of the Coulomb forces and by taking into account the renormalization of the single-particle energies due to the interactions with the other charged carriers.

The many-body interactions between carriers in heavily doped and highly excited semiconductors are known to have important effects on the physical properties of the carrier gas. this is quite apparent from optical and electrical experiments on a diverse range of systems varying from fundamental studies of electron-hole droplets through to efforts to develop better injection lasers, solar cells, and bipolar transistors. There is now a good understanding of these effects which has resulted from the early theoretical work on many-body effects in the high-density electron gas and, more recently, from the extensive range of experiments and calculations carried out on a variety of semiconductor systems. However, a good understanding should not be confused with a satisfactory and accessible quantitative description. For example, the concentrations of carriers in semiconductor systems that are studied in experiments are often such that the accuracy, or even the validity, of the many-body theory is in question. Even when

the basic aspects of the many-body formalism are accepted, the calculation of numerical results requires a nontrivial computational effort, as well as the incorporation of the approximations made necessary by the realities of the semiconductor band structure, such as anisotropic, nonparabolic, multiple energy bands.

It is possible to produce large, equal concentrations of electrons and holes in intrinsic semiconductor system by optical excitation and electronic injection. The many-body theory can be applied to the description of the electron-hole plasma. The valence and conduction bands, as well as the total bandgap narrowing, are calculated by Abram.[1]

The optical absorption and emission experiments of Casey *et al.* and their subsequent interpretation by Casey and Stern[2] constitute a thorough and comprehensive study of the optical properties of heavily doped GaAs at room temperature. The latter paper is also a useful source of references of earlier optical studies. Casey and Stern used a Hybrid Kane/Halperin and Lax model and suitably modified optical matrix elements to calculate the absorption and emission spectra of n- and p-type GaAs. The bandgap narrowing due to many-body effects was then deduced by comparing the theoretical and experimental absorption spectra. For p-type samples with hole concentrations varying between 1.2×10^{18} cm^{-3} and 1.6×10^{19} cm^{-3}, Casey and Stern find a simple relation between the bandgap narrowing due to many-band effects alone, ΔE_g, and the hole concentration p:

$$\Delta E_g = -1.6\times10^{-8}\, p^{1/3}$$

where ΔE_g is measured in electron volts and p in inverse cubic centimeters. No comparable result is quoted for n-type material. There are problems in measuring the change in bandgap in a heavily doped semiconductor by using optical absorption. The high density of carriers that exist in either the valence or the conduction band precludes absorption transitions involving state close to the edge of the occupied band. The result is the so called Moss-Burstein shift[3] of the absorption edge away from the energy of the fundamental gap. To deduce the gap it is essential to have a theoretical model which involves a description of the local electronic structure and

carrier distribution.

Recently, group III nitride semiconductors have attracted much attention as a material for fabricating blue and ultraviolet light-emitting diodes and lasers. Light emitting diodes based on InGaN/AlGaN heterostructures have achieved practical level.[4] More recently, successful fabrication of electrically pumped III-V nitride lasers have been reported.[5] But such material and related opto-electrical devices are still in preliminary stage, and many physical mechanisms affecting their active medium behavior are not understood in detail.

Many body effects in highly excited semiconductors have been studied intensively both experimentally and theoretically for many years,[6-9] and it is well known that many body Coulomb interactions between the carriers will lead to energy band renormalization or narrowing. Due to the large exciton binding energy, effective electron mass, and wide band gap of group-III nitride compounds, the effect of many body Coulomb interactions are expected to be more important.[7] A red shift of the peak of stimulated emission spectra for optically pumped GaN-based materials has been observed by different authors.[11-13] This red shift may be interpreted as strong many body effects overcoming a relatively small band filling effect. The investigations of many body effects are generally carried out using optical pump method and is concentrated mainly on GaAs-based materials, with few studies on GaN-based materials.[15-17]

In this section the band gap narrowing arising from many body interactions in the electron-hole plasma of current injected InGaN/AlGaN surface light emitting diode (SLED) is investigated. The dependence of electroluminescence on the injected current density has also been investigated. A luminescence line-shape analysis has been used to extract the essential parameters such as carrier density and the renormalized gap of the current pulse injected InGaN/AlGaN SLED.

4.2 Experiment and discussion

The SLEDs, comprised of $In_{0.06}Ga_{0.94}N$/AlGaN double heterostructures with Zn and Si-doped n-type active layer, are prepared by metalorganic chemical vapor deposition (MOCVD) on a sapphire (0001) substrate. The dark spot density in the samples were about 3×10^7 cm^{-2}. The details of the device fabrication conditions, structure and characteristics were described in previously reported results,[18] but our samples had no optical feedback.

The SLEDs were mounted on a copper heat sink, and operated in pulsed mode with pulse width of 100 ns at a frequency of 1 kHz. Figure 4-1 shows the surface emitting spectra measured at various injected currents (The similar emitting spectra were obtained in other samples also, The best luminescence efficiency has investigated here). A broad emission band at around 2.8 eV, which may be due to the free to bound acceptor or donor-acceptor pair recombination,[19] tends to saturate as the injected current increases and the band edge recombination emission at around 3.26 eV becomes more and more intense. The saturation of the broad emission at around 2.8 eV may be due to the limited impurity concentration. With an increase in the injected current, a clear red shift of the low energy edge, along with a broadening and a shift in peak energies of the emission spectra is observed. These phenomena can be caused by heating effect or many body effects. By fitting to the high energy tail of the measured spectra, with Boltzman factor $\exp\left[-\left(h\nu - E_g\right)/kT\right]$, the carrier temperature T can be obtained; here $h\nu$ is photon energy, E_g is the band gap energy and k is the Boltzman factor.[20] Although not shown here, when the high energy tail of the spectra was plotted as a function of photon energy on a logarithmic scale, it gave a constant temperature for all the injected current levels, which was close to bath temperature. Moreover, no shift in the peak energy of the spectra is observed with increasing current pulse frequency. Therefore, the red shift of the low energy edge and broadening of the emission spectra can be attributed to the many body effects, and not due to the heating effect.

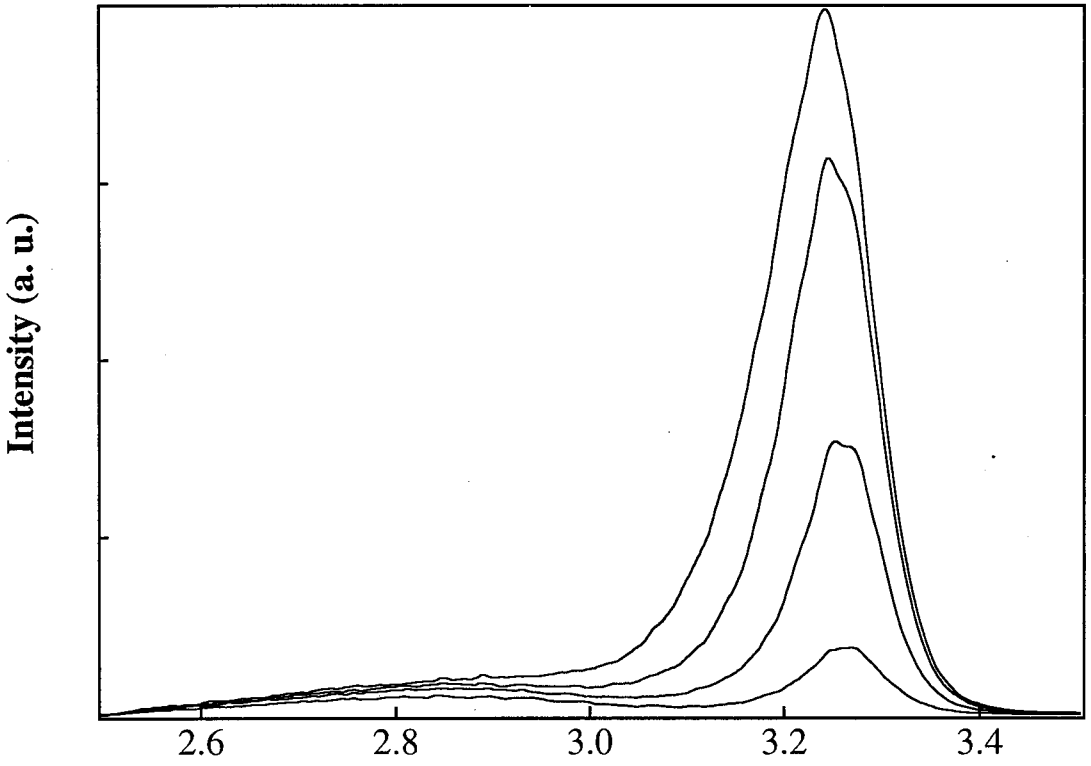

Fig. 4-1 The experimental emission spectra as function of photon energy at different injected currents of (from bottom to top) 0.4, 1, 2, and 3 A.

As no evidence of stimulated emission has been seen in measured emission spectra, so we tacitly assume that stimulated emission was negligible in our experiment. Similar to PL spectra the luminescence are described by the following intensity relation:[18]

$$I(h\nu) \propto \iint D_e(E_e)D_h(E_h)\delta(E_e - E_h - h\nu)dE_e dE_h \qquad (4\text{-}1)$$

where $D_{e,h}(E)$ are the number of electrons (holes) per unit energy range and unit volume (density of states times Fermi distribution function), which assumes the red shift of the low energy edge to be due to collision broadening of the electron and hole states, and is given by:[19-22]

$$D_e(E) \propto \frac{1}{2\pi}\int_0^{\infty} \frac{\Gamma(E_1)}{(E-E_1)^2 + (\Gamma(E_1)/2)^2} \frac{(E_1)^{1/2}}{1+exp[(E_1 - E_F^e)/kT]} dE_1 \qquad (4\text{-}2)$$

For the parameter Γ of the Lorentzian function, we take Landsberg's expression.[20] The fit parameters are the quasi-Fermi energies $E_F^{e,h}$ of electrons and holes, broadening parameter Γ_0 which is included in Γ and the renormalized gap E_g'. The carrier density is obtained from the relation:

$$n = \int_{-\infty}^{+\infty} D_e(E)dE \qquad (4\text{-}3)$$

In our calculation, reabsorption effects are not considered for the following reasons. Firstly, in surface light emitting diodes, the reabsorption is very small and the spectra will resemble that of PL. Secondly, absorption coefficient corresponding to photons of lower energies is smaller than that corresponding to higher energies. Thirdly, lower energy states of the conduction and valence bands being almost occupied under strong excitation, reabsorption mainly takes place on the higher energy side of photon energy and has little effect on the low energy edge. Since the renormalized band gap is determined by lower energy side of the spectra, reabsorption will have little effect on the calculated results of band gap narrowing.

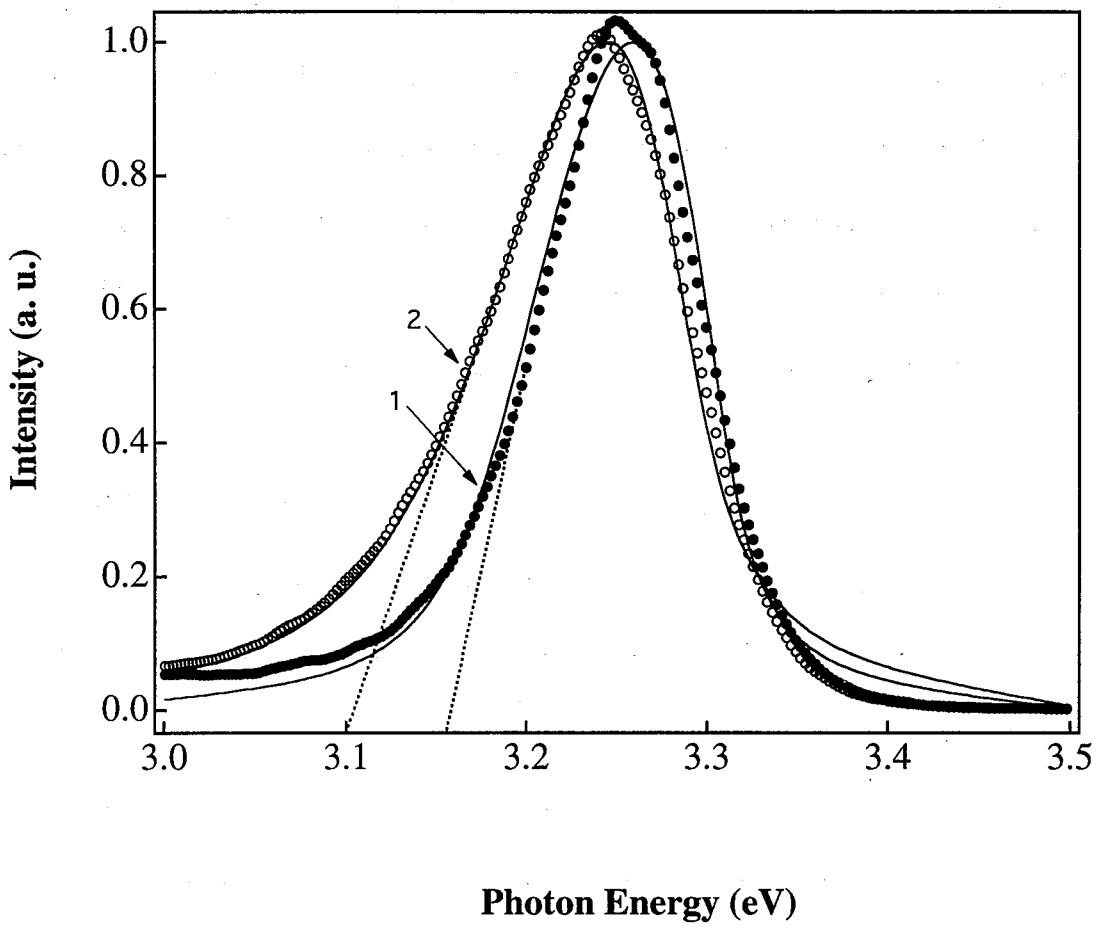

Fig. 4-2 Normalized emission spectra of InGaN/AlGaN diode with two different injected current, (1) 1 A; (2) 3 A. The symbols are experimental data, and the solid curves represent theoretical results. The broken line in lower energy side is used to obtained E_g' according to Tarucha's method.

Results of the line shape fitting are shown in Fig. 4-2. Theoretical fits are in very good agreement with the measurements. A decrease in the renormalized band gap E_g' with increasing injected current is clearly observed. According to Tarucha *et al.*[26] the renormalized band gap can also be determined by lower energy side of the spectra, and the red shift of the band gap can be directly approximated by an intercept of the tangent at half the peak intensity of lower energy side. However this method gives only relative red shift of the band gap, not the exact renormalized band gap. The results obtained by the two methods are shown in Fig. 4-3, which indicates similar injected current dependence of renormalized band gap E_g'. A red shift of around 92 meV of the low energy edge has been found as the pulsed injected current increased from 400 mA to 4000 mA.

The band gap narrowing due to many body interactions can be calculated theoretically considering the exchange energy of the electron-electron and hole-hole interactions. Stern showed simple relation between the band gap narrowing and the carrier density:[27]

$$E_g' = E_g + A(n^{1/3} + p^{1/3}) \qquad (4\text{-}4)$$

where n and p are electron and hole concentration, respectively, and A is a constant.

The above equation is valid only if the ratio of intercarrier spacing to the electron Bohr radius in the crystal is less than unity, and the carrier-impurity interaction, carrier-carrier Coulomb interactions are not considered. Our experimental results are in good agreement with above relation, with A = -5.8 $\times 10^{-8}$ eV/cm, and E_g = 3.324 eV (the band gap energy of $In_{0.06}Ga_{0.94}N$ at room temperature), which is shown in Fig. 4-4. Experimental observations of bandgap narrowing for GaAs[28] and InP[29] can also be described by the above relation, with a relatively smaller value of A, -2.15 $\times 10^{-8}$ and -2.25 $\times 10^{-8}$ eV/cm, respectively. The large value of A for InGaN may indicate stronger many body effects than that for GaAs and InP. Zhang *et al.* have also reported similar relation of band gap with carrier concentration for optical pump on GaN, however, with a much smaller value (-1.1 $\times 10^{-8}$ eV/cm) of the constant term A.[17] In our opinion, they may have overestimated the value of carrier concentration by taking a small value

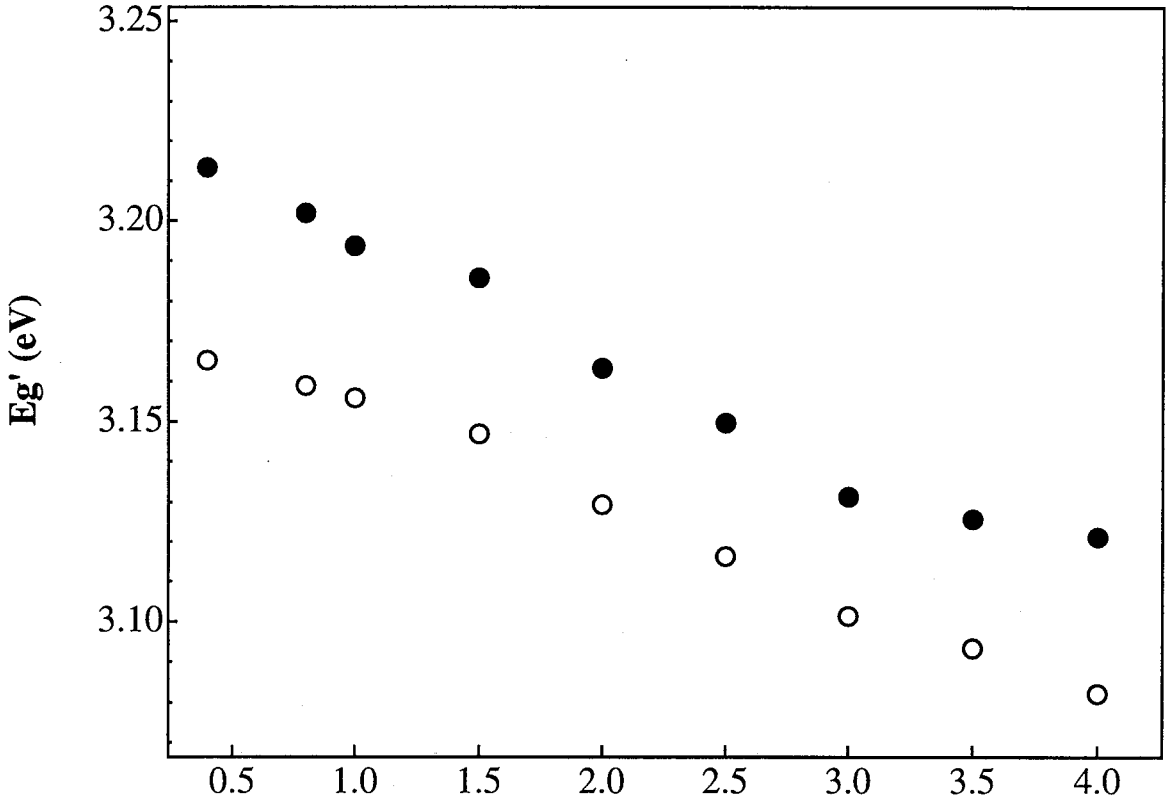

Fig. 4-3 Injected current pululsed dependence of the renormalized E_g'. The dots are extracted from spectra line-shape fitting, and circles are obtained by Tarucha's method.

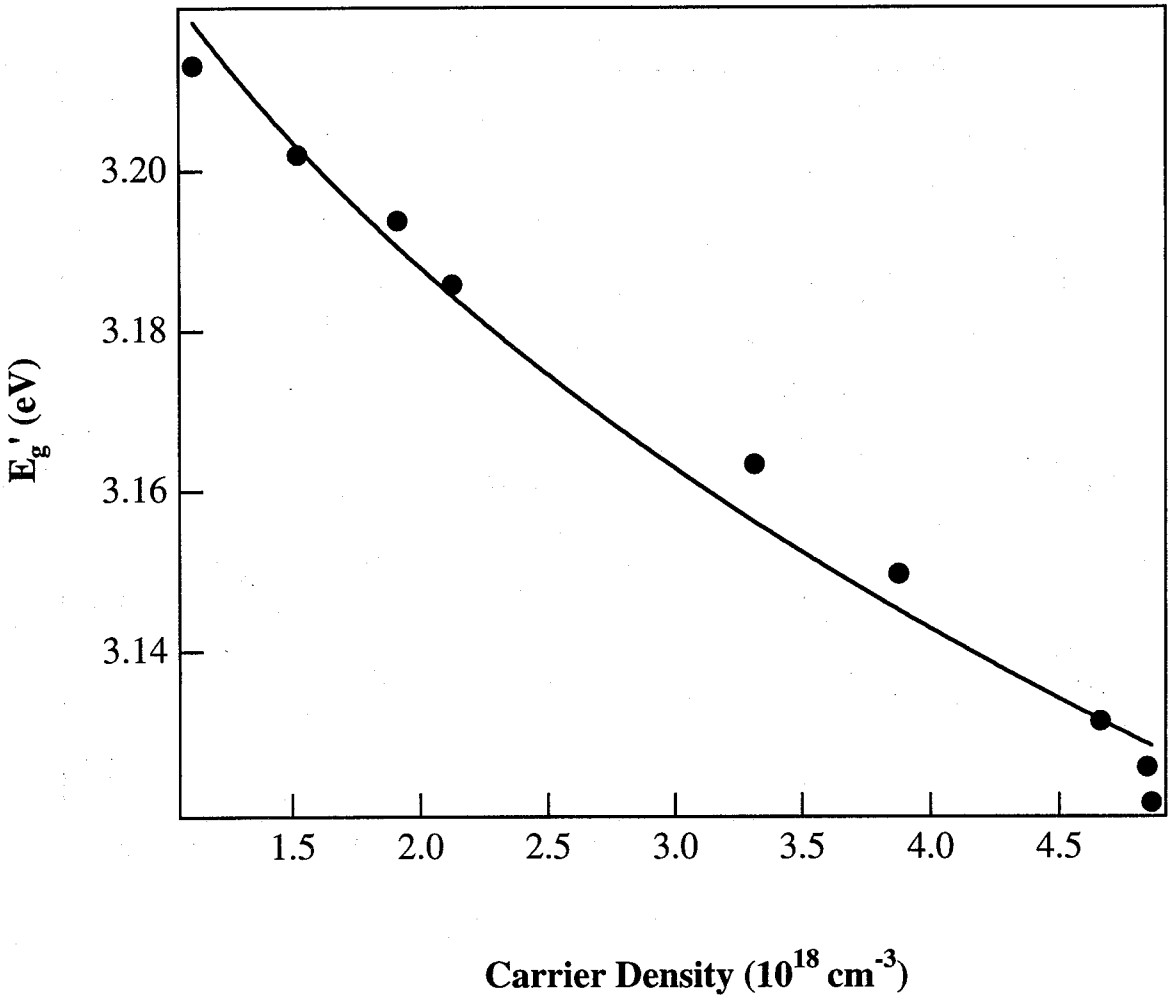

Fig. 4-4 Renormalized E_g' as a function of carrier density. The dots represent spectra shape-line fit results, and the solid curve is for that calculated ones using $E_g' = E_g - 5.8 \times 10^{-8} (n^{1/3} + p^{1/3})$ (eV) with E_g=3.324 eV.

for A, because they did not consider the carrier density pinning effect which occurs in the strong stimulated emission case.

Semiconductor lasers based on group III nitrides compounds are interesting because they operate in the viable wavelength region. The band gap of the nitrides ranges from 1.8 eV of InN to 6.3 eV of AlN, making them promising candidates for light emitting diodes (LEDs) and laser diodes (LDs). These has been a growing interest in the optical properties of nitride films due to several recent advances.

In several recent papers describing theoretical investigations, the gain medium is treated as either an inhomogeneously broadened ensemble of two-level systems, representing excitons, or electron-hole plasma. The gain spectra can be obtained from unamplified spontaneous emission, from which electroluminescence is measured, and the gain is calculated via a transformation that results from the Einstein relationship between spontaneous and stimulated transitions.

The relationship between spontaneous and stimulated transition rates is easily derived by requiring that the radiation density obtained at radiative equilibrium is the same as that obtained at thermodynamic equilibrium. This result is easily extended to give the relationship between gain and spontaneous emission. which, for a semiconductor, is

$$\alpha(h\nu, \Delta E_F) \propto I(h\nu, \Delta E_F)\exp\left[(h\nu - \Delta E_F)/kT\right] \tag{4-5}$$

$$g(h\nu, \Delta E_F) \propto I(h\nu, \Delta E_F)\left\{1 - \exp\left[(h\nu - \Delta E_F)/kT\right]\right\} \tag{4-6}$$

where $\alpha(h\nu)$ is the absorption coefficient, $g(h\nu)$ is the gain as a function of photon energy hv, $I(h\nu)$ is the spontaneous emission density, and ΔE_F is the separation of the electron and hole quasi-Fermi levels. In fact, only relative values for $I(h\nu)$ are determined experimentally. To obtain absolute values for the gain, it is necessary to measure $I(h\nu)$ and, in addition, the

separation of quasi-Fermi levels ΔE_F, the quasi-Fermi level separation can be determined as following:

1) the quasi-Fermi level separation ΔE_F is simply the junction voltage. An estimate of this voltage can be obtained from the measured device contact voltage by subtracting the series voltage drop. The series resistance of the device is obtained from the slope of the current-voltage curve at higher injection current condition.

2) ΔE_F can be determined from the best fits to the measured spontaneous emission with our model. Since the width of the spontaneous emission is a sensitive function of ΔE_F, these values are more accurate than 1).

ΔE_F is a more fundamental parameter than current. A value of ΔE_F can be found for each current, so we write the detected luminescence intensity as $I(h\nu)$. The changes in ΔE_F can be determined by the ratios of the luminescence intensities. From equation (4-5)

$$\frac{I(h\nu,\Delta E_{F1})}{I(h\nu,\Delta E_{F2})}=\frac{\alpha(h\nu,\Delta E_{F1})}{\alpha(h\nu,\Delta E_{F2})}\exp\left(\frac{\Delta E_{F1}-\Delta E_{F2}}{kT}\right) \qquad (4\text{-}7)$$

Carrier injection modifies the absorption edge, but for photon energies sufficiently far above the absorption edge, the absorption coefficient is independent of carrier injection and therefore is independent of ΔE_F for the high energy edge side; so equation (4-7) can be samplies to

$$\frac{I(h\nu,\Delta E_{F1})}{I(h\nu,\Delta E_{F2})}=\exp\left(\frac{\Delta E_{F1}-\Delta E_{F2}}{kT}\right) \qquad (4\text{-}8)$$

The high-energy tails of the spontaneous emission spectra differ only by a constant factor $\exp[(\Delta E_{F1}-\Delta E_{F2})/kT]$.

The low- and high-intensity spectra are compared by sliding the logarithmic plots of spontaneous emission intensity until the high-energy tails nearly coincide. Within errors of about 10 K, we find no change in carrier temperature when the LED is increased in current from 100 mA to 4000 mA.

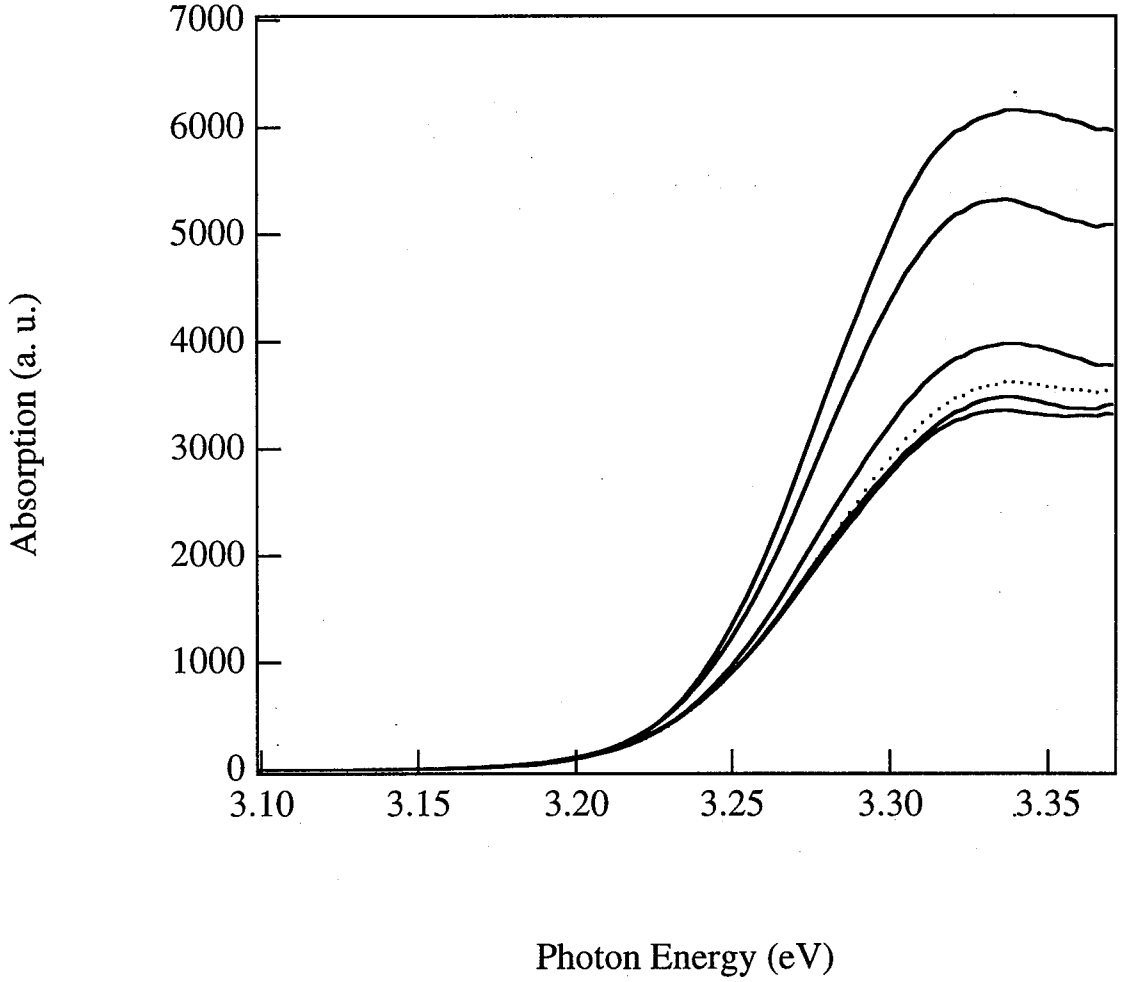

Fig. 4-5 The calculated absorption spectra as functions of photon energy at different injected currents of (the current increasing from top to bottom) 1.5, 2.0, 2.5, 3.0, 3.5, and 4.0 A.

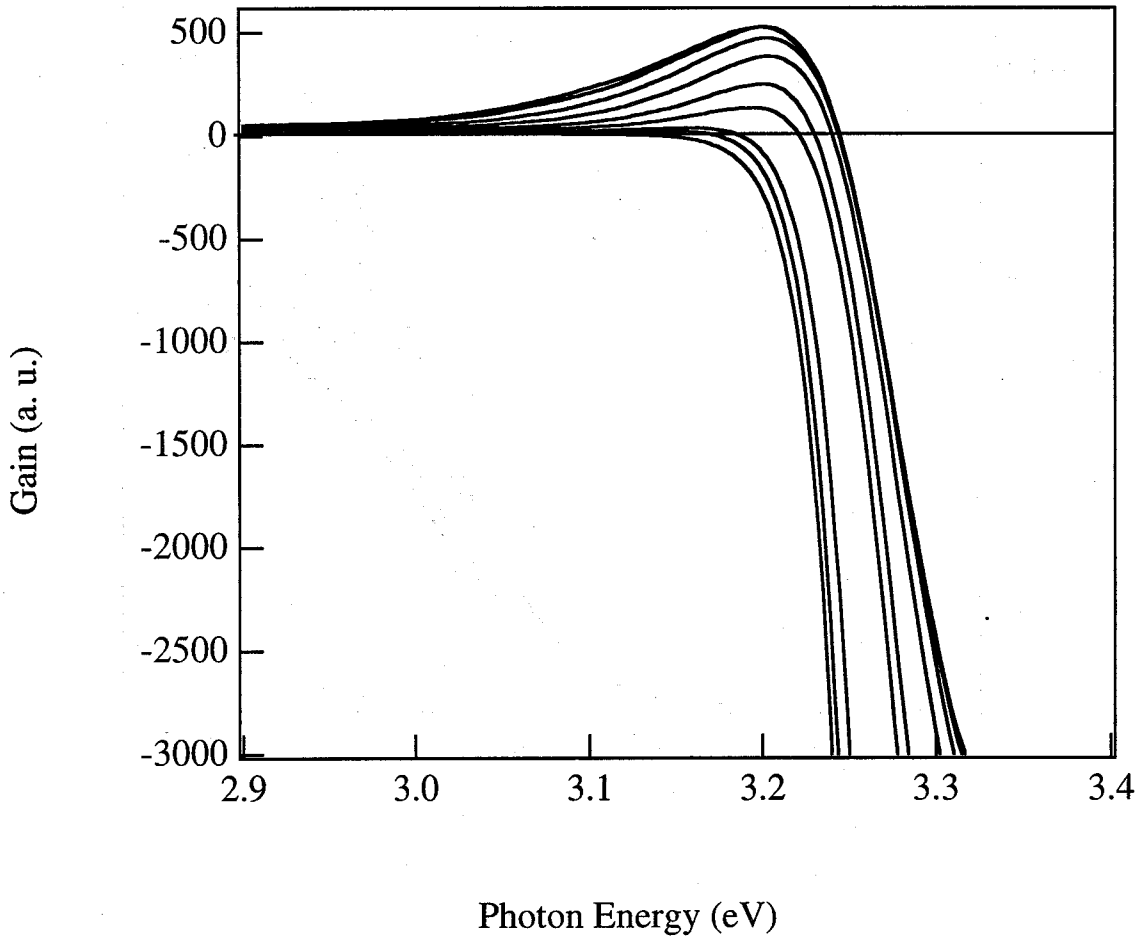

Fig. 4-6 The calculated gain spectra as functions of photon energy at different injected currents of (the current increasing from bottom to top) 0.6, 0.8, 1.0 1.5, 2.0, 2.5, 3.0, 3.5, and 4.0 A.

The spontaneous emission spectrum of our LED is shown in Fig. 4-1. The spontaneous emission spectra are converted into absorption and gain spectra in Fig. 4-5 and Fig. 4-6. As the injection intensity increased, one clearly observes:

1) a decrease of the absorption, and an increase of the net gain amplitude,

2) a pronounced shift to higher energies of the point where the net gain changes to absorption, and

3) a shift to lower energies of the low energy side of the net gain spectra.

This behavior observed above, can be explained by band filling and by many body effects of electron-hole system at high carrier densities which lead to a high energy shift of the chemical potential and a bandgap shrinkage, respectively.

4.3 Conclusion

In summary, we have measured and analyzed emission spectra of a current injection InGaN/AlGaN surface emitting diode. A clear red shift of the low energy edge with increasing injected current has been observed, and is attributed to many body effects. The carrier density and band gap narrowing are extracted by emission spectra line-shape fit using Landsberg model which includes many body effects causing collision broadening of the electron and hole states. The band gap change can be described well in proportion to the 1/3 power of the carrier density, and further supports our supposition that band gap narrowing is caused by many body effects which is more effective phenomenon for group III nitrides.

Reference

[1]R. A. Abram, G. J. Rees and B. L. H. Wilson, Adv. Phys. **27**, 799 (1978).

[2]H. C. Casey and F. Stern, J. Appl. Phys. **47**, 631 (1976).

[3]T. S. Moss, Proc. Phys. Soc. **B67**, 775 (1954).

[4]S. Nakamura, T. Mukai, and M. Senoh, Appl. Phys. Lett., **64**, 1687 (1994).

[5]S. Nakamura, M. Senoh, S. I. Nagahama, N. Iwasa, T. Yamada, T. Matsushita, H. Kiyoku, and Y. Sugimoto, Jpn. J. Appl. Phys. **35**, L74 (1996).

[6]H. Haug, and S. Schmitt-Rink, Progr. Quant. Electr. **9**, 3 (1984).

[7]H. Schweizer and E. Zielinski, J. Lumin. **30**, 37 (1985)

[8]R. Cingolani, K. Ploog, A. Cingolani, C. Moro, and M. Ferrara, Phys. Rev. B **42**, 2893 (1990).

[9]S. Schmitt-Rink, D. S. Chemla, and D. A. B. Miller, Adv. Phys. **38**, 89 (1989).

[10]W. W. Chow, A. Knorr and S. W. Koch, Appl. Phys. Lett. **67**, 754 (1995).

[11]S. T. Kim, H. Amano, and I. Akasaki, Appl. Phys. Lett. **67**, 267 (1995).

[12]X. H. Yang, T. J. Schmidt, W. Shan, and J. J. Song, Appl. Phys. Lett. **66**, 1 (1995).

[13]T. Tanaka, K. Uchida, A. Watanabe, and S. Minagawa, Appl. Phys. Lett. **68**, 976 (1996).

[14]S. Kurai, Y. Naoi, T. Abe, S. Ohmi, and S. Sakai, Jpn. J. Appl. Phys. **35**, L77 (1996).

[15]R. Cingolini, M. Ferrara and M. Lugara', Solid State Commun. **60**, 705 (1986).

[16]X. Zhang, P. Kung, A. Saxler, D. Walker, T. C. Wang, and M. Razeghi, Appl. Phys. Lett. **67**, 1745 (1995).

[17]X. Zhang, P. Kung, A. Saxler, D. Walker, and M. Razeghi, J. Appl. Phys. **80**, 6544 (1996). [18] T. Egawa, Y. Murata, T. Jimbo and M. Umeno, Electron. Lett. **32**, 486 (1996);

[18]T. Egawa, H. Ishikawa, T. Jimbo and M. Umeno, Appl. Phys. Lett. **69**, 830 (1996).

[19]S. Nakamura, T. Mukai, and M. Senoh, Appl. Phys. **76**, 8189 (1994).

[20]M. H. Pilkuhn and W. Schairer, in *Handbook on semiconductors* **4**, Device Physics, edited by C. Hilsum (Elsevier Science Publisher B. V., Amsterdam, 1992), p.668.

[21]A. L. Mcwhorter, Solid State Electron. **6** , 417 (1963).

[22]P. T. Landsberg, Phys. Stat. Sol. **15**, 623 (1966).

[23]P. T. Landsberg and D. J. Robbinns, Solid State Electron. **28**, 137 (1985).

[24]R. W. Martin and H. L. Störmer, Solid State Commun. **22**, 523 (1977).

[25]P. T. Landsberg, Proc. Phys. Soc. A **62**, 806 (1949).

[26] S. Tarucha, H. Kobayashi, Y. Horikoshi, and H. Okamoto, Jpn. J. Appl. Phys. **23**, 874 (1984).

[27]F. Stern, J. Appl. Phys. **47**, 5382 (1976).

[28]J. Shah, R. F. Leheny and C. Lin, Solid State Commun. **18**, 1035 (1976).

[29]M. Bugajski and W. Lewandowski, J. Appl. Phys. **57**, 521 (1985).

Chapter 5 Opto-thermal Properties of GaN

5.1 Introduction

The group III nitride-based semiconductors have been become as the most promising material for short-wavelength light-emitting diodes and lasers, as for coherent light source, they are crucial for high density optical read and write technologies.[1] That may make them the best potential optical devices to complete the optical computation. Optical bistable device has many potential advantage for applications in optical logic and signal processing.[2] Optical bistability and related nonlinear phenomena have been studied in several semiconductor small band gap materials such as InSb[3] InAs[4] and CdHgTe[5] exhibit particularly large nonlinearities of electronic origin at photon energies close to the band gap energy. Thermally induced refractive index changes in semiconductors have also gained increasing interest. Optical bistability has been achieved in this way under band gap resonant conditions in Si,[6] GaAs,[7] ZnSe,[8] and ZnS.[9, 10] This is the first report of this kind on GaN to our knowledge.

Two classes of bistability have received prominent attention, namely those associated with refractive index changes brought about (1) by carrier generation (optoelectronic) and(2) by sample temperature changes (Optothermal). The overall problem of semiconductor bistability is as follows. The material is described by a refractive index n, interband absorption α_i, and additional absorption (due for example to the created free carriers) α_p. Radiation I_1, at frequency ω, is incident on the material in a cavity formed either by the natural surface reflectivities or by external partial mirrors/coatings. The consequent internal irradiance $I(\omega)$ must then be determined and also the transmitted and reflected irradiances. This is the cavity feedback problem and it may involve steady-state or time dependence, plane-wave or nonuniform illumination.

The internal irradiance generates ΔN carriers and a temperature change ΔT. For steady state, one is therefore concerned with the carrier recombination mechanisms (trap, radiative, Auger, surface recombination) and/or the thermal losses. The band structure and the state populations alter as a consequence. Given an understanding of all absorption processes, the changes $\Delta\alpha_i$ and $\Delta\alpha_p$ may be determined and, in turn, the refractive index change Δn calculated by Kramers-Kronig transformation. A thermal expansion of Fabry-Perot cavity may also be significant.

5.2 Background and theory

The cavity optical path length (nD) plays the dominant role in determining the Fabry-Perot response. For nonlinear system, the path length change is given by

$$\frac{\Delta(nD)}{nD} = \frac{1}{n}\frac{\partial n}{\partial N}\Delta N + \left(\frac{1}{n}\frac{\partial n}{\partial T} + \frac{1}{D}\frac{\partial D}{\partial T}\right)\Delta T$$

The first term, the electronic refractive contribution, is determined by the refractive index cross section (per generated carrier pair), $\partial n/\partial N = \sigma_n$. It will be not considered here. The second term is the therm-optic contribution and is in general an order of magnitude larger than the final, thermal-expansion term. $\partial n/\partial T$ can be calculated using a well known Kramers-Kroning transformation of the band edge absorption:[14]

$$\Delta n(h\nu) = \frac{\hbar c}{\pi}\int_0^\infty \frac{\alpha(E_g + \Delta E_g) - \alpha(E_g)}{(h\nu')^2 + (h\nu)^2} d(h\nu')$$

This relations allow us to transform the problem of determining the behavior of the refractive index to the problem of finding the behavior of the absorption coefficient. Fortunately, we have experimental data for the absorption coefficient near the absorption edge of most semiconductors, and we can in many cases determine the nonlinear behavior near absorption

edge using this relation.

For bistability the change in optical length, induced by the internal radiation, I, must be at least of order $\lambda_V/2F$, where λ_V is the vacuum wavelength and F the cavity finesse. A low absorption is needed to attain a high finesse, but at the same time there must be sufficient absorption to give the required steady-state concentration or temperature changes. We shall concentrate on direct-gap semiconductors, under near-resonant operation.

5.3 Experiment and Discussion

In order to predict accurately the performance of a candidate material for optothermal nonliearities devices, a knowledge of the thermo-optical coefficient (dn/dT) is needed. In this section, we present the results of the nonlinearity near the absorption edge caused by thermally induced refractive index changes of GaN epilayer grown by metal-organic chemical-vapor deposition (MOCVD). It is found that this material is having a very large thermo-optical coefficient compared to other semiconductors. Spectroscopic ellipsometry (SE) was used to determine the refractive index of GaN layer over a large wavelength region for different measured temperatures. The measured parameters of SE, Δ and Ψ, are extremely sensitive to overlayers on the surface of the material such as a natural oxide layer or a rough layer, which is a major drawback in the accurate determination of optical constants of studied materials. Fortunately, GaN has a very good chemical stability, the oxide layer is negligible for this material and MOCVD growth technique can obtain very flat surface.

The sample, used in the experiment, was 2.4 μm undoped GaN epitaxial layer grown on a mirror polished sapphire (0001) substrate with a low temperature growth 30 nm GaN buffer layer by MOCVD.[11] The thickness of the epilayer was measured by scanning electron microscope (SEM). The sample was heated on a hot plate, and the temperature of the sample was

measured with a W-Re thermocouple. When the measurement was made in the atmosphere, it was found that the thermocouple probe does not accurately give the temperature of the sample. This discrepancy is probably due to the poor contact between the probe and sample. In order to get the correct temperature, the measurement was carried out with oil drop on the contact point of sample and probe. Because oil has greater thermal mass and heat transfer capability than that of air, sample and thermocouple is at equilibrium with the oil rather than the heat radiation field.

Due to the high refractive index of GaN, the interface of GaN with air has a reflection coefficient of about 40%, and the same with sapphire is about 20%, so these interface from a Fabry-Perot etalon. When a light beam radiates the sample, the interference effects will be observed. Figure 5-1 shows the SE experiment data of Ψ for two different measurement temperatures. Each set of measurement from 25°C to 160°C gives a statistically large number of Ψ values which are then averaged. The changes of absorption edge and location of interference fringes can be clearly seen.

The basic equation for the interference fringes is[12, 13]

$$\beta = m\pi = \frac{4\pi d\left(n^2 - \sin^2\phi\right)^{1/2}}{\lambda} \qquad (5\text{-}1)$$

where β represents the phase difference, λ is the wavelength of monochromatic light in vacuum, d and n are the thickness and refractive index of GaN layer, respectively, ϕ is the angle of the incidence, and m is an even (or odd) integer for maxima and an odd (or even) integer for minima.[12] Therefore, using the equation (5-1) the refractive index and thickness of GaN layer can be obtained. In this method the refractive index of GaN layer can be determined without knowing the refractive index of sapphire. Because the results are only related with extreme locations in the interference fringes of SE data with Ψ. Because of absorption, measurement error increases with increasing energy close band gap, above band gap the interference fringe can not be clearly seen, so the refractive index can not be obtained in this region. Figure 5-2 shows the calculated results of the refractive index for three different temperatures. We find that there is

rapid dispersion of the refractive index near the band edge The refractive index increases with the temperature increasing, and a large change of refractive index has been observed at photon energies close to the band gap energy. The thickness (2.56 μm) of the GaN is also obtained which matches closely with that obtained by SEM. Due to the very small thermal expansion coefficient of GaN ($\Delta a/a = 5.59\times10^{-6}$ K^{-1}), the change in light path length by thermal expansion is less one order of magnitude than the thermo-optical contribution.[14] Therefore, the effect of thermal expansion was neglected in our calculation .

Refractive index n is measured for varying the temperature conditions in the vicinity of two temperature regions, 25°C and 100°C. The derivation of n, $dn(h\nu)/dT$, at the two regions are obtained from the n vs T plots. For the calculation of the thermo-optical coefficient $dn(h\nu)/dT$, a cubic spline interpolating technique was used to obtain the refractive index with respect to the desiring wavelength. The temperature dependence of GaN thermo-optical coefficient $dn(h\nu)/dT$ in the band-edge region was shown in Fig. 5-3. The value of $dn(h\nu)/dT$ increases with temperature increasing, resulted from the shrinkage of band gap with temperature increasing.

In room temperature the GaN demonstrated a very large thermo-optical coefficient (2.6×10^{-3} K^{-1}) at 0.365 μm, compared to other semiconductors in which the thermal dispersive bistability has been reported. e.g. Si: 2.4×10^{-4} at 1.06 μm.[7] GaAs 7×10^{-4} at 0.85 μm.[8] ZnS 1.4×10^{-4} at 0.514 μm,[10] ZnSe 5×10^{-4} at 0.476 μm.[9] E. Ejder[15] has reported a experiment result of (1/n) $dn/dT = 2.6\times10^{-5}$ K^{-1} which measured at long-wavelength below room temperature. This value is two times lesser than our result (5.4×10^{-5} K^{-1}) at long-wavelength (2.5 eV). An empirical relation has proposed by Moss[16] for the temperature dependence of n in long-wavelength region:

$$\frac{dn}{dT} = n\frac{1}{4E_g}\frac{dE_g}{dT} \qquad (2)$$

where E_g is the band gap. Inserting a value of 6.7×10^{-4} eV/K^{-1} (Ref. 17) for dE_g/dT and using E_g=3.42 eV,[18] a value $(1/n)\ dn/dT = 4.9\times10^{-5}$ K^{-1} is obtained which can compare with our experimental result. The large thermo-optical coefficient close the band gap energies, may be

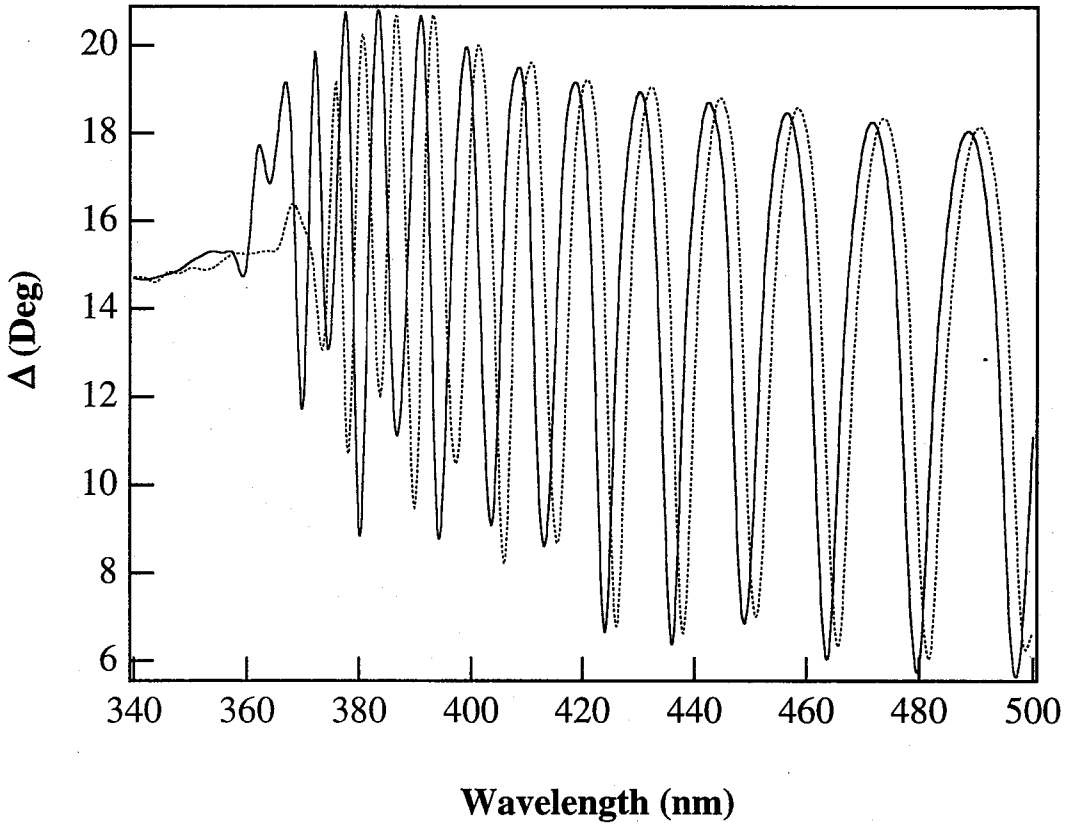

Fig. 5-1 Solid and dotted line show the values of Ψ for 25 and 100 °C respectively.

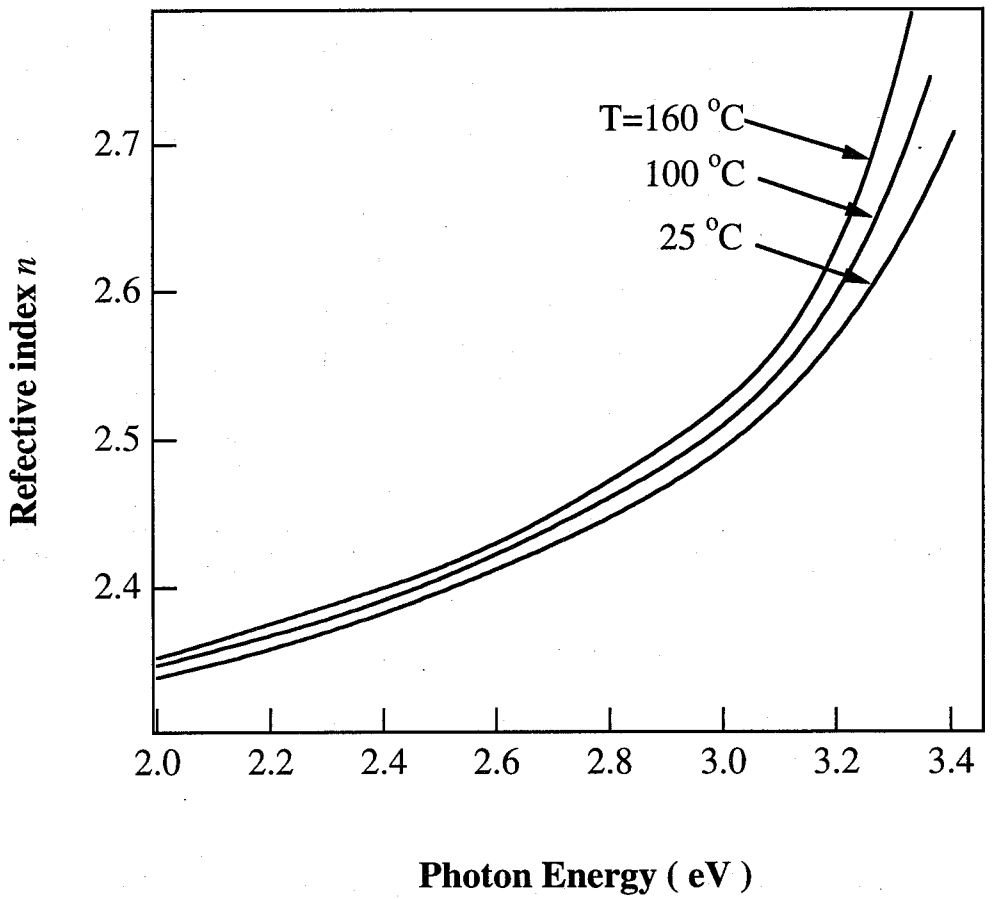

Fig. 5-2 Refractive index of GaN for different temperatures.

caused by a steep band gap absorption edge of GaN.

Harris *et al.*[19] gave an empirical dispersion of d*n*/d*T* near the band gap for several material:

$$\frac{dn}{dT} = a\left(\frac{\lambda^2}{\lambda^2 - \lambda_g^{\,2}}\right)^b \qquad (5\text{-}3)$$

The equation relates the value of d*n*/d*T* to the wavelength and energy gap of semiconductor materials investigated. We used the above equation to fit our values of d*n*/d*T*, the results are also shown in Fig. 5-3 and the fitting parameters are given in Table I. Even though the experimental results are well agreed with the empirical relationship, the correct band gap energy is not obtained.

Close to the band gap edge, the nonlinear index is determined by the temperature dependence of the edge itself and the background thermo-optical coefficient as follows:[14]

$$\frac{dn}{dT} = \frac{\partial n}{\partial E_g}\frac{\partial E_g}{\partial T} + \left(\frac{\partial n}{\partial T}\right)_b \qquad (5\text{-}4)$$

The coefficient $\frac{\partial n}{\partial E_g}$ is obtainable using a Kramers-Kroning (K-K) transformation of the band gap edge absorption[14]

$$\Delta n(h\nu) = \frac{\hbar c}{\pi}\int_0^\infty \frac{\alpha(E_g + \Delta E_g) - \alpha(E_g)}{(h\nu')^2 + (h\nu)^2} d(h\nu') \qquad (5)$$

The measured values of d*n*/d*T* may be qualitatively compared to calculated results of K-K transformation as a consistency check. For this, we used experimental absorption coefficient as in our previous report.[13] Assume a rigid shift of the absorption coefficient with the change of band gap, and take $\partial E_g/\partial T$ = 0.67 meV K^{-1}, here, binomial smooth and cubic spline interpolating techniques were used for the experimental absorption coefficient. The experimental (25°C) and calculated results are shown in Fig. 5-4. The integral is truncated at E=2.95 eV and

E=3.54 eV. The values of $\Delta\alpha$ outside this range is negligible, and they do not contribute to the integral. The qualitative agreement is observed.

Table I. Values of Constants in Empirical Dispersion Relationship (Ref.18)

	a (10^{-6}/°C)	b	λ_g
25 °C	1.804	3.801	0.337
100 °C	9.65	2.135	0.352

5.4 Conclusion

The SE technique was used to measured refractive index, then thermo-optical coefficient (dn/dT) of GaN can be obtained with the measured results made in different temperature. The experimental results demonstrated very large thermo-optical nonlinearity for this material at the band gap edge, since this material has large absorption coefficient and edge. The value of dn/dT increase with increasing temperature, resulted from that the energy gap and absorption coefficient do not vary linearly with temperature. Using Kramers-Kronig transformation, we calculated the theoretical value of dn/dT, which has good consistency with the experimental results.

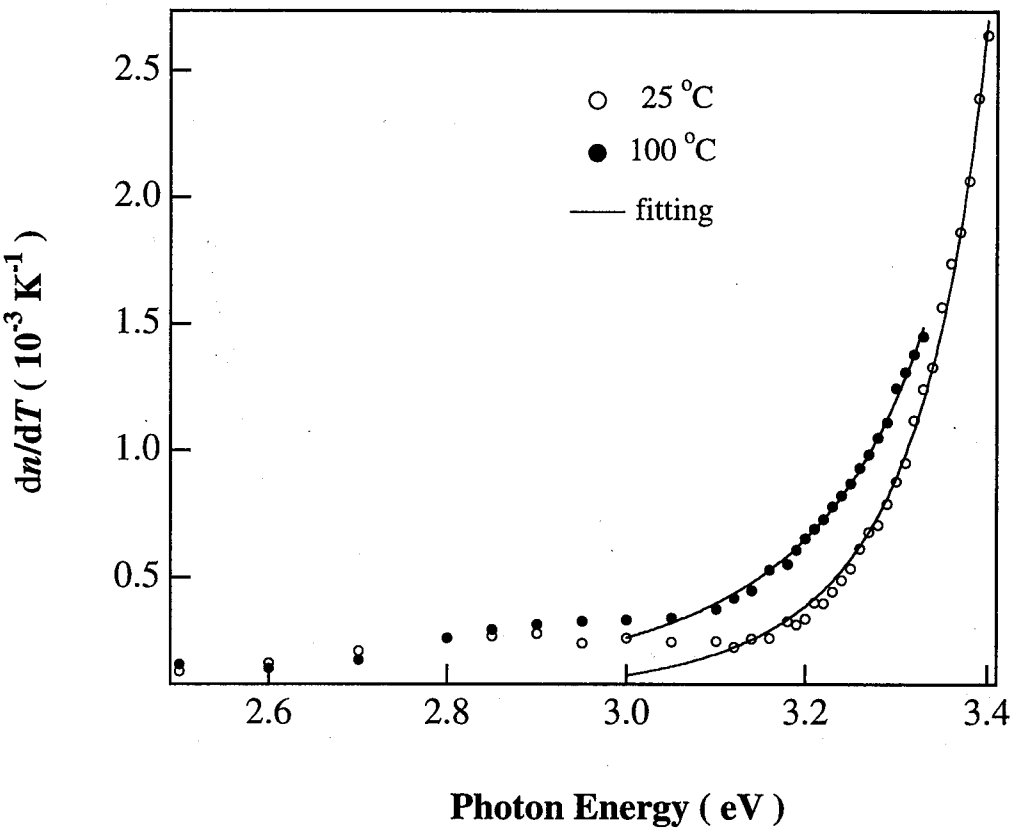

Fig. 5-3 Thermo-optic coefficient of GaN in the band edge region for different temperatures

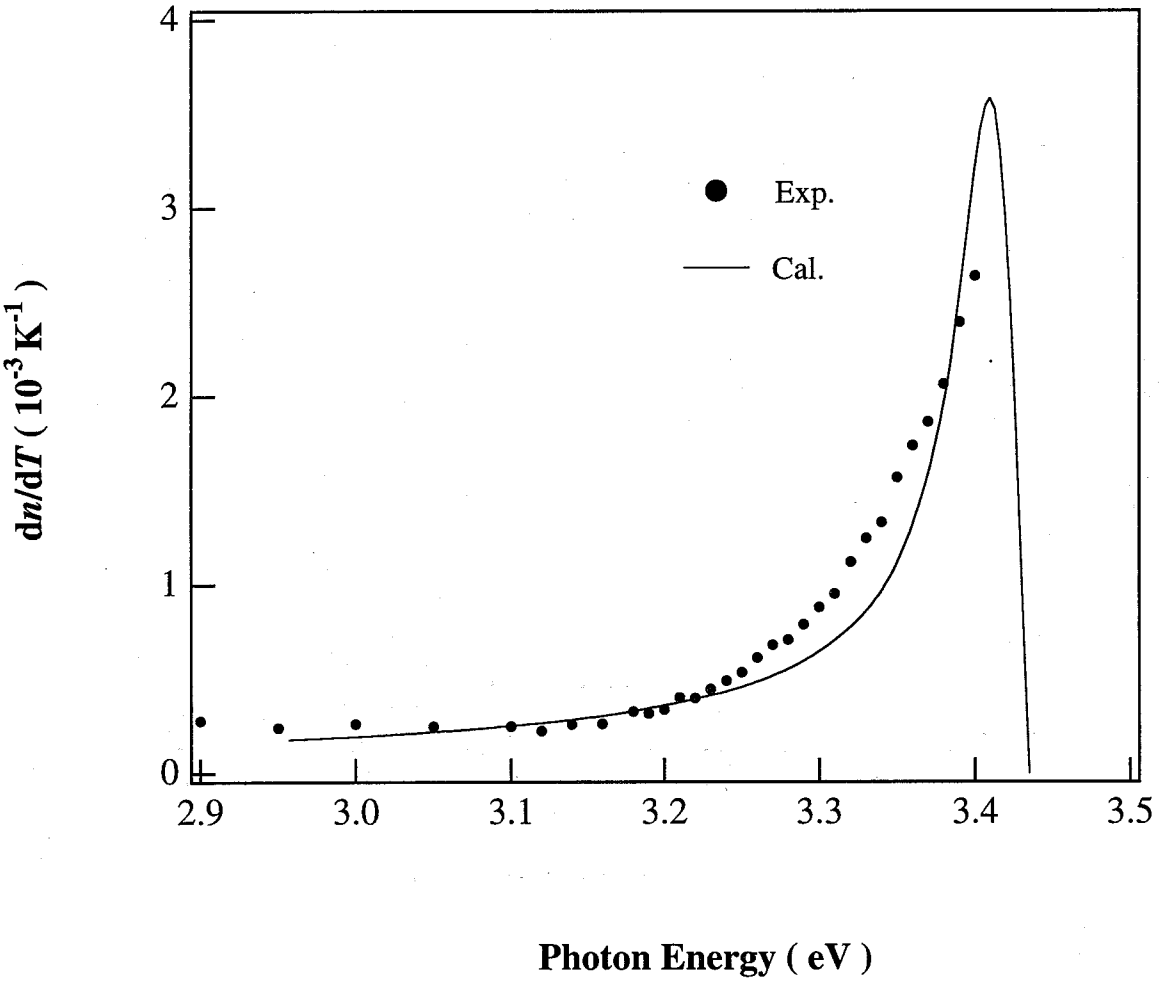

Fig. 5-4 Photon energy dependence of thermo-optical coefficient of GaN. In the calculation of solid line, the experimentally obtained absorption coefficients (smoothed and interpolated for caculation) were used.

References

[1]S. N. Mohammad, A. A. Salvader, and H. Morkoc, Proceedings of the IEEE. **83**, 1306 (1995)

[2]N. Peyghambarian and H. M. Gibbss, in *Optical Nonlinearities and Instabilities in Semiconductors*, edited by H. Haug (Academic Press, INC., London, 1988), p295.

[3]A. C. Walker, F. A. P. Tooley, M. E. Prise, J. H. G. Mathew, A. K. Kar, M. R. Taghizadeh and S. D. Smith, Phil. Roy. Soc. London, **A313**, 249 (1984).

[4]C. D. Poole and E. Garmire, Appl. Phys. Lett. **44**, 363 (1984).

[5]J. R. Hill, G. Parry and A. Miller, Opt. Commun. **43**, 151 (1983).

[6]N. Peyghambarian and H. M. Gibbss, Opt. Eng. **24**, 68 (1985).

[7]H. J. Eichler, Opt. Commun. **45**, 62 (1983).

[8]H. M. Gibbs, S. L. McCall, T. N. C. Venkatesan, A. C. Gossard, A. Passner and W. Wiegmann, Appl. Phys. Lett. **45**, 357 (1984).

[9]S. D. Smith, J. G. H. Mathew, M. R. Taghizadeh, A. C. Walker, B. S. Wherrett and A. Hendry, Opt. Commun. **51**, 357 (1984).

[10]G. R. Olbright, N. Peyghambarian and H. M. Gibbss, H. A. M. Macleod and F. V. Milliger, Appl. Phys. Lett. **45**, 357 (1984).

[11]H. Ishigawa, K. Nakamura, T. Egawa, T. Jimbo and M. Umeno, Jpn. J. Appl. Phys. **37**, L7 (1997).

[12]G. Yu, G. Wang, H. Ishikawa, M. Umeno, T. Soga, T. Egawa, J. Watanabe and T. Jimbo, Appl. Phys. Lett. **70**, 3209 (1997).

[13]G. Yu, H. Ishikawa, T. Egawa, T. Soga, J. Watanabe, T. Jimbo and M. Umeno, Jpn. J. Appl. Phys. **36**, L1029 (1997).

[14]B. S. Wherret, A. C. Walker, and F. A. P. Tooley, in *Optical Nonlinearities and*

Instabilities in Semiconductors, edited by H. Haug (Academic Press, INC., London, 1988), p239.

[15]E. Ejder, phys. stat. sol. (a) **6**, 445 (1971).

[16]T. S. Moss, *Optical Properties of Semiconductors*, Butterworths, London 1961.

[17]D. L. Camphausen and G. A. N. Connell, J. Appl. Phys. **42**, 4438 (1971).

[18]H. P. Maruska and J. J. Tietjen, Appl. Phys. Lett. **15**, 327 (1996).

[19]R. J. Harris, G. T. Johnston, G. A. Kepple, P. C. Krok and H. Mukai, Appl. Opt. **16**, 436 (1977).

Chapter 6. Summary

The Principle motivation of the present work was to explore electronic properties of undoped p-type GaSb, which has some ambiguous knowledge in present reports, and basic physics properties of GaN, which is in the early stage of development and many physical mechanism affecting their active medium behavior are not understood in detail.

In Chapter 1, we briefly reviewed the present status of the two materials, GaSb and GaN. The purpose of this work are also described.

In Chapter 2, the MBE apparatus and growth process of GaSb were described in detail. It was found that mirror-like surface of GaSb epilayer can be obtained over large substrate temperature range (460~530°C), and Sb/Ga flux ratios (5~10). High quality epilayers with excellent morphology were grown.

In Chapter 3, A careful investigation of the electrical properties of GaSb epitaxial layer MBE-grown on SI-GaAs substrate was described, and a detailed model was used to discuss the properties of GaSb. Variable Hall-effect measurements have been carried out on several undoped GaSb samples grown by MBE. It is found that the electrical properties of GaSb epilayers strongly depend on growth temperature. High unintentionally doped impurity concentration and high compensation ratio are observed for lower and higher growth temperature. On such samples the impurity conduction may be a dominant conduction mechanism at low temperatures, and common method of curve fitting to concentration vs. $1/T$ curve may give wrong results; therefore, the analysis of mobility vs. T data has been carried out. In addition, the electrical transport properties of GaSb are analyzed in energy dependent relaxation scattering processes, and it is demonstrated that device usage of GaSb is limited by high unintentionally doped impurity concentration as well as high compensation ratio.

In this Chapter, the PL and I-V characteristics of GaSb were also studied. The spectrum are

typical of GaSb grown under all antimony stable conditions and show the various transitions which have been observed in good quality materials. The dominant recombination mechanism proceeded via the residual acceptor A , at 777.5 meV, for all the samples. It was found that the spectra obtained from higher growth temperature, a series bound exciton transitions and recombination at the neutral acceptor level, and a exciton bound to donor (D) is clearly seen, this mean our samples, which grown at higher temperature, have very good crystal quality, because the bound energy is very small for this material. For the sample growth at 500°C, a strong and narrow A peek is observed, increasing the growth temperature, all transition peaks become weak and broaden. The temperature dependent I-V characteristics in bulk of GaSb p-n junctions are measured and analyzed. At reverse bias, the tunnel current is dominant at a large temperature region. The large leakage current is mainly caused by tunnel current. The diffusion current surpasses the tunnel current at high temperature and high bias of both forward and reverse voltage.

In Chapter 4, we have measured and analyzed emission spectra of a current injection InGaN/AlGaN surface emitting diode. A clear red shift of the low energy edge with increasing injected current has been observed, and is attributed to many body effects. The carrier density and band gap narrowing are extracted by emission spectra line-shape fit using Landsberg model which includes many body effects causing collision broadening of the electron and hole states. A redshift of around 92 meV of low energy edge is obtained as injected current increases from 400 to 4000 mA. The band gap change can be described well in proportion to the 1/3 power of the carrier density, and further supports our supposition that band gap narrowing is caused by many body effects which is more effective phenomenon for group III nitrides.

In Chapter 5, the thermo-optical coefficient (dn/dT) of GaN is obtained with SE technique. In room temperature the GaN demonstrated a very large thermo-optical coefficient ($2.6\times 10^{-3}\ K^{-1}$) at 0.365 μm (near band edge), compared to other semiconductors in which the thermal dispersive bistability has been reported. e.g. Si: 2.4×10^{-4} at 1.06 μm, GaAs 7×10^{-4} at 0.85 μm, ZnS 1.4×10^{-4} at 0.514 μm, ZnSe 5×10^{-4} at 0.476 μm. The large thermo-optical coefficient close the band

gap energies, may be caused by a steep band gap absorption edge of GaN. The value of dn/dT increase with increasing temperature, resulted from the shrinkage of band gap with temperature increasing. Using Kramers-Kronig transformation, we calculated the theoretical value of dn/dT, which has good consistency with the experimental results.